3D LIDAR-based ground segmentation

Article · November 2011

DOI: 10.1109/ACPR.2011.6166587

Tongtong Chen
National University of Defense Technology

Daxue Liu
National University of Defense Technology

3D LIDAR-based Ground Segmentation

Chen Tongtong, Dai Bin, Liu Daxue
College of Mechatronic Engineering and Automation
National University of Defense Technology
Changsha, China
chentongtong5208@gmail.com

Zhang Bo, Liu Qixu
Trucks and Ships Military Delegate Bureau
General Armament Ministry
Beijing, China

Abstract—**Obtaining a comprehensive model of large and complex ground typically is crucial for autonomous driving both in urban and countryside environments. This paper presents an improved ground segmentation method for 3D LIDAR point clouds. Our approach builds on a polar grid map, which is divided into some sectors, then 1D Gaussian process (GP) regression model and Incremental Sample Consensus (INSAC) algorithm is used to extract ground for every sector. Experiments are carried out at the autonomous vehicle in different outdoor scenes, and results are compared to those of the existing method. We show that our method can get more promising performance.**

Keywords-ground segmentation; point clouds; polar grid map; Gaussian process; INSAC

I. INTRODUCTION

Autonomous driving in outdoor environments has become the focus of autonomous vehicle in recent years. In order to complete the autonomous driving task safely and quickly, the promising object classification results are crucial. Given a set of 3D points acquired by LIDAR, the final goal of segmentation is to attribute the points to a set of candidate object classes. In the context of autonomous vehicle, this segmentation capability is not only essential for high-level tasks like scene understanding and planning, but also be used for planning. The ground segmentation in 3D point clouds often is the first step in the autonomous perception tasks, such as objects classification, dynamic object detection and tracking and so on. The results of the ground segmentation will directly influence the later classification.

In this paper we present an improved ground segmentation method for 3D LIDAR point clouds. The proposed algorithm keeps all 3D points acquired for the sensor, and builds on prior approach to generate a circular polar grid map of radius 50 meters as [4], and then it is divided into many sectors. The 1D GP regression [1] and INSAC algorithm is used to fit the ground model in every sector. This method results in an accurate segmentation in different kinds of scenes, and we demonstrate it with our autonomous vehicle (see Fig.1) which is equipped with a Velodyne HDL-64E S2 Laser.

The rest of the paper is organized as follows. An outline of the related work is given in the next section. In section □, this paper describes the ground segmentation approach in detail, followed by some experimental results in section □. The experiments are carried out at autonomous vehicle in different outdoor scenes, and results show the performance of the presented method. Finally a conclusion of this paper and an outline of the future work are given in section □.

Figure 1. Autonomous vehicle used in this paper, equipped with Velodyne HDL-64E S2 Laser.

II. RELATED WORK

With rang scanning devices becoming standard equipment in autonomous vehicle, a lot of researches have been carried out over the last years concerning the ground segmentation of 3D LIDAR point clouds. In general, the ground segmentation approach includes cell-based method in grid elevation map [2-3], line-based method in polar grid map [4], and fitting plane method [5-8].

Cell-based method in grid elevation map was widely used by many teams at the 2007 DARPA Urban Challenge competition in order to segment the point clouds and to detect the obstacle on the track. Height difference is computed between the maximum and the minimum height of the returns falling for each cell in a min-max elevation map [2], and if it is less than a pre-defined threshold, then the cell is declared ground. B. Douillard et al use a mean elevation map to extract the ground surface, if the largest gradient between the cell and its neighbors exceeds a threshold, the cell is identified as obstacle [3].

Line-based method in polar grid map: M. Himmelsbach et al divided the polar grid map into some sectors, and used the line extraction algorithm in [10] to represent the ground model in every sector [4], such as Incremental algorithm, ANSAC algorithm, Hough-transform.

Fitting plane method: for many applications, the ground is known to be flat. In that case, the ground segmentation algorithm should determine planar surfaces. Joseph Lam et al solved the ground segmentation problem by applying plane ANSAC algorithm followed by a least square fit on 3D data [5]. G. Vosselman et al use 3D Hough transform to describe every non-vertical plane [6]. S. Vasudevan et al use the dependent Gaussian processes for data fusion in the context of large scale

Supported by the National Natural Science Foundation of China (Grant No.90820302)

terrain modeling, and demonstrate the use of the non-stationary kernel in [7]. B. Douillard et al use 2D Gaussian process regression and INSAC algorithm to segment the ground in elevation map [8], and they get good results.

The approach most similar to our work is [4] and [8]. For every sector, line fits are used to model the ground in [4], which can represent the flat ground very well, but for the rough ground, its performance is not accurate. Reference [8] used 2D Gaussian process regression and INSAC algorithm in whole elevation map and provided close to real-time performance. In order to improve the computational efficiency, the approach presented in this paper use 1D Gaussian process regression which has the superior modeling capability [7] for every sector, and the cost time is in proportion as the number of the sectors. We can achieve real-time performance of doing ground segmentation of point clouds in full 3D.

III. GROUND SEGMENTATION ALGORITHM

Instead of establishing complex neighborhood relations [3] and computing the height difference [2] in every cell as commonly done in ground segmentation, in our method we partition the data in a way that allows the ground point to be estimated by 1D Gaussian process regression. Together, the partitioning and 1D Gaussian process can be considered an approximation of the ground surface segmentation algorithms with 2D Gaussian process.

In this section, the detailed algorithm for ground segmentation is presented. We begin the description of the proposed method with some notes on data acquisition and polar grid map representation in [4] and go into details of Gaussian process regression afterward. We finally show how to use 1D Gaussian process regression and INSAC algorithm [8] to segment ground in 3D point clouds.

A. Data Acquisition and Polar Grid Map Representation

The method in this paper is shown to segment the ground, given the large clouds of 100 000 points delivered by Velodyne HDL-64E S2 on top of the autonomous vehicle at rate of 10 Hz. The HDL-64E S2 Laser outputs UDP Ethernet packets. Each packet arrives in a data payload of 1206 bytes that consists of 12 blocks of 100-byte firing data followed by six bytes at the end of each packet, and it is rate to provide usable returns up to 120 meters [9]. These packets are collected for the time of one sensor revolution in what we call a frame [4].

With the translation and rotation transform (Extrinsic Calibration of the 3D LIDAR), a frame data will be denoted by the set $P=\{p_1,p_2,\dots p_n\}$ with 3D point $p_i=\{x_i,y_i,z_i\}$ given by their Euclidean coordinate with respect to the vehicle-coordinates system with origin O in the front of the vehicle. In Order to simplify the 2D segmentation problem into a 1D regression problem, we partitioned the 3D point clouds into a circle polar grid map of the radius $R=50$ meters and divided it into M sectors, as shown in Fig.2. The point p_i whose length $Op_i=\sqrt{x_i^2+y_i^2}>R$ is omitted, the other points is mapped into the sectors according to its angle with the positive x axis. We use $\Delta\alpha=2\pi/M$ to represent the angle every sector covers. The index to a sector which a point belongs to is denoted by $S(p_i)$, and it can be easily calculated by

$$S(p_i)=\frac{sgn(y_i)\bullet acos(x_i/Op_i)+2\pi\bullet\varepsilon(-y_i)}{\Delta\alpha} \quad (1)$$

Where $sgn(y_i)$, $\varepsilon(y_i)$ are sign function and unit step function, respectively. The symbol P_s represents the set of all points that are mapped to the same sector S_s

$$P_s=\{p_i\in P\,|\,S(p_i)=s\} \quad (2)$$

However, this only gives us an ordering of points with respect to their angular component. We still cannot apply 1D Gaussian process regression to describe the ground in every sector as our expectation.

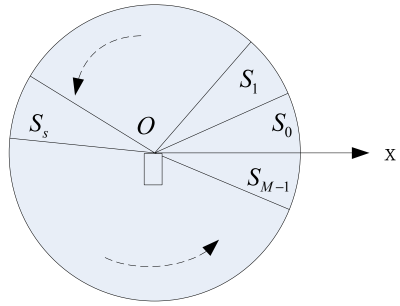

Figure 2. Dividing the polar grid map into M sectors of equal size, the rectangle in the center represents the vehicle.

In order to modeling the ground in the sector with 1D Gaussian process regression, we divide each sector into N bins. The j^{th} bin b_j in a sector covers the range from $r_j^{\min}$ to $r_j^{\max}$. The point $p_i\in P_s$ maps to bin b_j^s if and only if

$$r_j^{\min}\le Op_i<r_j^{\max} \quad (3)$$

We use the symbol $P_{b_j^s}$ to denote the set of all points that map to the j^{th} bin in sector s. Once all points have been mapped to a sector and a corresponding bin, the method in [4] is applied to convert the 3D points to 2D. Given a set $P_{b_j^s}$ of 3D points, we can simply define a new set of 2D point $P_{b_j^s}{'}$ as

$$P_{b_j^s}{'}=\left\{p_i{'}=(Op_i,z_i)\,|\,p_i\in P_{b_j^s}\right\} \quad (4)$$

Obviously, the point-to-bin mapping is not one to one, because the 3D point clouds are sparse. The set $P_{b_j^s}'$ may contain more than one point or no points at all.

Our approach models the ground in every sector, for any set $P_{b_j^s}'$ that is not empty in the sector s , $s = 0 \cdots M$, we choose the point $p_i' \in P_{b_j^s}'$, $j = 1 \cdots N$ with the lowest z_i to form the set PG_s as it is most likely to lie on the ground.

$$PG_s = \{p_i' = (Op_i, z_i) \mid p_i' \in P_{b_j^s}', z_i = min(z), j = 1 \cdots N\} \quad (5)$$

B. Gaussian Process regression

The goal for the ground segmentation of 3D point clouds in outdoor environments is to establish a binary labeling of all points indicating whether a point belongs to the ground or not. As we are targeting both the urban and country scenarios, the ground model must be suited to describe both flat and up-and-down terrain. A Gaussian process is a collection of random variables, any finite number of which have a joint of Gaussian distribution [1]. It is a non-parametric Bayesian, continuous representations that provides a powerful basic for modeling spatially correlated and probability uncertain data. A Gaussian process $f(x)$ is completely specified by its mean function $m(x)$ and covariance function $k(x, x')$. In the context of the problem at hand, each $x \equiv Op$, and $f(x) \equiv z$. For notational simplicity we will take the mean function $m(x)$ to be zero, although this need not be done. The covariance function $k(x, x')$ models the relationship between the random variables corresponding to the given data. In this paper, the squared-exponential covariance function in one dimension is used, and it has the following form

$$k(x, x') = \sigma_f^2 exp(-\frac{1}{2\ell^2}(x - x')^2) + \sigma_n^2 \delta \quad (6)$$

Where ℓ is the length-scale, σ_f^2, σ_n^2 are the signal variance and the noise variance respectively. These free parameters $\ell, \sigma_f^2, \sigma_n^2$ constitute the hypeparameters of the covariance function.

Gaussian process regression use the fact that the joint distribute of the training outputs z , and test outputs f_* according to the prior is

$$\begin{bmatrix} z \\ f_* \end{bmatrix} \sim N\left(0, \begin{bmatrix} K(X,X) + \sigma_n^2 I & K(X,X_*) \\ K(X_*,X) & K(X_*,X_*) \end{bmatrix}\right) \quad (7)$$

If there are n training points and n_* test points then $K(X, X_*)$ denotes the $n \times n_*$ matrix of the covariance evaluated at all pairs of the training and test points, and similarly for the other entries $K(X, X), K(X_*, X_*)$ and $K(X_*, X)$. The key predictive equations for Gaussian process regression take the form

$$\begin{aligned} \bar{f}_* &= K(X_*,X)\left[K(X,X)+\sigma_n^2 I\right]^{-1} z \\ V[f_*] &= K(X_*,X_*) - K(X_*,X)\left[K(X,X)+\sigma_n^2 I\right]^{-1} K(X,X_*) \end{aligned} \quad (8)$$

C. Gaussian process Increment Sample Consensus

The Gaussian Process Increment Sample Consensus (GP-INSAC) algorithm is an iterative approach to probabilistic, continuous ground surface estimation for sparse 3D data sets cluttered by non-ground object [8]. It maintains the properties of Gaussian process terrain modeling techniques and endows with an outlier rejection capability. The ground segmentation algorithm is summarized in algorithm 1.

Algorithm 1: ground segmentation

Input : $P = \{p_1 \cdots p_n\}$
Output : $model$
Parameters: $t_{data}, t_{model}, M, B_s$
1: $PG = PolarGridMap(P)$
2: **for** i=0: $M-1$ **do**
3: $s_{new} = s_p = \varnothing$
4: $s_{new} = seed(PG_i, B_s)$
5: **while** size (s_{new}) > 0 **do**
6: $s_p = s_p \cup s_{new}$
7: $s_{new} = \varnothing$
8: $model = regression(GP, s_p)$
9: $test = PG_i - s_p$
10: $s_{new} = eval(model, test, t_{data}, t_{model})$
11: **end while**
12: **for** j=1: N **do**
13: $segment(model, P_{b_j^i}', T_g)$
14: **end for**
15: **end for**

The algorithm starts with a set of 3D point clouds, and comprises five steps: polar grid map representation, seed calculation, Gaussian process regression, ground point evaluation, and ground segmentation.

Once the 3D points are maps to corresponding sectors, an initial seed of the likely ground points in the sector is calculated using the function $seed$. In this paper, the points with z less than the pre-defined threshold are chosen as seeds or inliers. Gaussian process regression uses these seeds as training data to fit a model (using $regression$ function), and evaluates the remaining data as test points (using $eval$ function), the INSAC uses the probabilistic model that estimate the uncertainly of their predictions. The parameter t_{model} specifies the threshold of the covariance of the test point, and the parameter t_{data} specifies the normalized proximity of the test point to its mean. Two rules are expressed by

$$\begin{aligned} & V(f_*) < t_{modle} \\ & \frac{z_i - f_*}{\sqrt{\sigma_n^2 + V(f_*)}} < t_{data} \end{aligned} \tag{9}$$

For the test points, they are classified inliers if and only if they satisfy both the rulers, otherwise they are classified outliers. Starting from the seed, inliers are accumulated per iteration, which performed until no more inliers are found. Fig.3 shows the result of GP-INSAC algorithm for a sector.

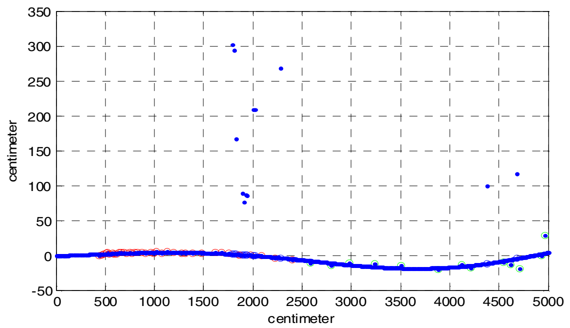

Figure 3. The GP-INSAC algorithm is running on the data set PG_4 in the 4th sector of the image (g) in Fig 6, the blue points are raw data, the red circles represent the seed points, and the green circles are inliers. The blue curve represents the ground in the sector.

For every sector, when we get the final model, the proximity height H_g of ground in every bin is estimated, the points p_i in the bin that satisfy the ruler $|z_i - H_g| \le T_g$ is classified ground, otherwise it belongs to obstacle (using $segment$ function).

IV. EXPERIMENTS

We have evaluated the proposed algorithm for many frames acquired by the HDL-64E S2 Laser mounted on our autonomous vehicle both in urban and countryside scenes. These scenes included the highway with some traffic, field road with some road-blocks, and the road with a slope. As no ground true information is available, a qualitative performance evaluation is conducted.

In our complementation, the polar grid map covers an area of radius 50 meters, and it is divided into $M = 360$ sectors, every sector is divided into $N = 160$ bins. In the GP-INSAC algorithm, the parameters were fixed $\ell = 0.3$, $\sigma_f^2 = 1.3298$, $\sigma_n^2 = 0.1$, $T_{model} = 0.5$, $T_{data} = 80.0$, $T_g = 30$.

Fig.4 shows some results of the ground segmentation in three different scenes compared to those obtained with method described in [2] and [4]. The images from left to right are results of our presented method, method in [4], and method in [2], respectively. The first row shows the highway scene with a vehicle, a cyclist and a pedestrian, our method (left) and the method (right) in [2] can get good performance, while some points (the red points in the green rectangle) were wrongly classified obstacles with the method in [4] (middle), because the vehicle disturbed the line fitting process in the corresponding sectors. The second row shows the field road scene with some road-blocks in front of the vehicle (red points), the method in [4] (middle) cannot segment the ground very well, such as the red points in the green rectangle, that is because the road surface is not flat, it is hard to fit a line in these sectors. The same thing happens to the method (right) in [2], the height differences on the left of the image (green rectangle) exceed the threshold because of the rough road surface (the gradient of the cell is large). The slope road scene is shown in the last row. Our method describes the slope road perfectly. The method in [4] (middle) and in [2] (right) cannot adapt the slope very well. In consequence, our method can describe various grounds very well, and the method in [4] and [2] can get good performance only on the flat ground.

V. CONCLUSION

We present an improved algorithm for ground segmentation for our autonomous vehicle equipped with Velodyne HDL-64E S2 Laser. With the method, we can segment the ground accurately. It is useful for object classification and dynamic obstacle detection and tracking. At the core of the algorithm are Gaussian process regression and INSAC algorithm. We demonstrated that our method achieve good segmentation results on data acquired in a variety of scenarios both in urban and countryside environments.

REFERENCES

[1] C. E. Rasmussen, and C. K. Williams, Gaussian processes for Machine Learning. the MIT press, England: Massachusetts Institute of Technology, 2006.

[2] S. Thrun and et al, "Stanley: The Robot that Won the DARPA Grand Challenge," Journal of Filed Robot (JFR), USA, pp. 661-692, June 2006.

[3] B.Douillard, J.Underwood, N. Melkumyan, S.Singh, S.Vasudevan, C. Brunner, and A. Quadros, "Hybrid Elevation Map: 3D Surface Models for Segmentation," IEEE International Conference on Intelligent Robots and System (IROS), 2010.

[4] M. Himmelsbach , Felixv. Hundelshausen, and H. J. Wuensche, "Fast Segmentation of 3D Point Clouds for Ground Vehicles," IEEE Intelligent Vehicles Symposium (IV), USA, pp. 560-565, June 2010.

[5] J. Lam, K. Kusevic, P. Mrstik, R. Harrap, and M.Greenspan, "Urban Scene Extraction from Mobile Ground Based LIDAR Data," 5th International Symposium on 3D Data, Visualization & transmission, France, pp. 1-8, May 2010.

[6] G.Vosselman, B. G. H. Gorte, G. Sithole, and T. Rabbani, "Recognising Structure in Laser Scanner Point Clouds," International Archives of Photogrammetry, Remote Sensing and Spatial Information Sciences, pp 33-38. 2004 .

[7] S. Vasudevan, F. Ramos, E. Nettleton, and H. D. Whyte, "Non-stationary dependent Gaussian processes for data fusion in large-scale terrain modeling," IEEE International Conference on Robotics and Automation (ICRA), China, pp. 1875-1882, May 2011.

[8] B. Douillard, J. Underwood, N. Kuntz, V. Vlaskine, A. Quadros, P.Morton, and A. Grenkel, "On Segmentation of 3D LIDAR Point Clouds," IEEE International Conference on Robotics and Automation (ICRA), China, pp. 2798-2805, May 2011.

[9] HDL-64E S2 User's manual, pp5.

[10] V. Nguyen, A. Martinelli, N. Tomatis, and R. Siegwart, "A Comparison of Line Extraction Algorithms using 2D Laser Rangefinder for Indoor Mobile Robotics," IEEE Internation Conference on Intellignet Robots and Systems (IROS), Canada, 2005.

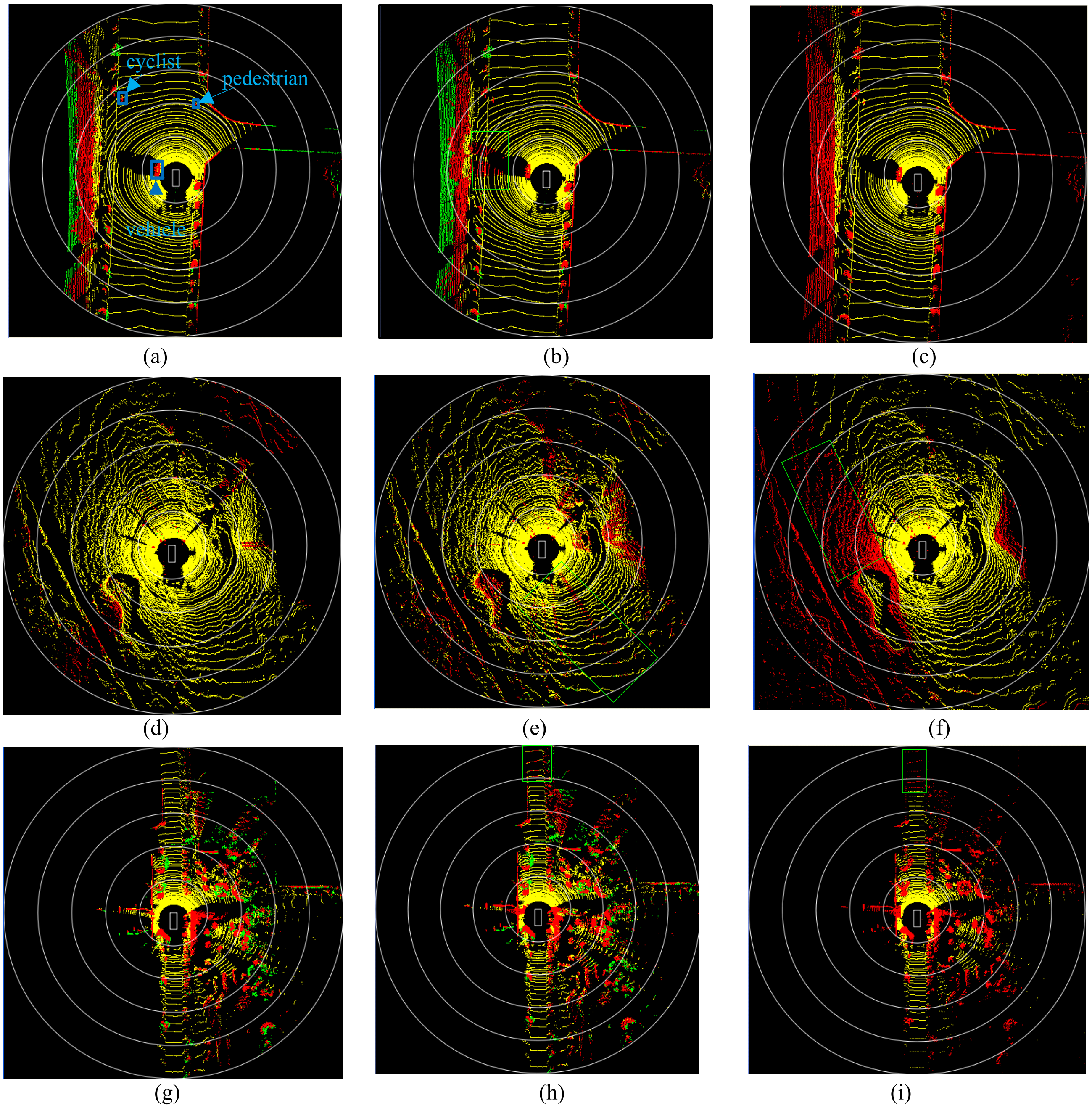

Figure 4. Segmentation results of our method (left column) in three different scenes, compared to the results of the methods in [4] (middle column) and in [2] (right column). The ground points are colored in yellow scales,while red points represent the obstalces, and the green points are overhanging objects.